Molecular Therapy
Methods & Clinical Development
Original Article

One-Step Fabrication of Bone Morphogenetic Protein-2 Gene-Activated Porous Poly-L-Lactide Scaffold for Bone Induction

Jingwen Xue,[1,2,4,5] Hang Lin,[1,2] Allison Bean,[1,2,6] Ying Tang,[1,2,7] Jian Tan,[1,2] Rocky S. Tuan,[1,2,3] and Bing Wang[2,3]

[1]Center for Cellular and Molecular Engineering, University of Pittsburgh School of Medicine, Pittsburgh, PA 15219, USA; [2]Department of Orthopaedic Surgery, University of Pittsburgh School of Medicine, Pittsburgh, PA 15219, USA; [3]McGowan Institute for Regenerative Medicine, University of Pittsburgh School of Medicine, Pittsburgh, PA 15219, USA; [4]School of Medicine, Tsinghua University, Beijing, 100084, China

Bone morphogenetic protein 2 (BMP2) is an efficacious inducer for the osteogenesis of mesenchymal stem cells (MSCs). Conventional applications of BMP2 have involved either the direct incorporation of BMP2 protein or ex vivo BMP2 gene transfer into stem cells prior to their transplantation. These approaches are able to promote bone formation to some extent; however, they are hampered by either the lack of stability and sustainability of BMP2 protein or the time-consuming and cost-prohibitive in vitro cell culture procedure. To overcome these limitations, we have developed a gene-activated poly-L-lactide acid (PLLA) scaffold with the encapsulation of recombinant adeno-associated viral (AAV) vector encoding a full-length cDNA of human BMP2 using an ice-based microparticle porogenization method that was recently developed. Results showed continuous release of AAV particles from the micropores of scaffolds for up to 1 week, subsequently transducing embedded human MSCs and producing functional BMP2. MSCs within scaffolds underwent efficacious osteogenesis, on the basis of osteoinductive gene expression and osteogenic differentiation, which resulted in robust new bone formation in vivo at 4 weeks. These findings show the potential of the technology toward developing clinical applications of a rapid, cost-effective, and potentially point-of-care approach for the repair of bone defects.

INTRODUCTION

Although bone is one of the most actively repaired tissues of the body, delayed union or non-union sequelae are observed in 10%–15% of the approximately 6.5 million bone fracture cases in the United States yearly.[1] In addition, osteoporotic fractures are common in the elderly population and occur in approximately 1.5 million fractures annually in the United States. Enhancement of bone regeneration is also required for the healing of large bone defects secondary to tumor or trauma and for treating fracture-related delayed unions or non-unions. Therefore, developing an efficacious technology for bone regeneration is of health importance to all age groups.

Clinically, autologous bone grafts have been considered the "gold standard" for the repair of bone defects, but this method is accompanied by donor site morbidity and is greatly restricted by tissue availability.[2] Bone tissue engineering using human mesenchymal stem cells (hMSCs) seeded in a porous, biodegradable biomaterial scaffold, such as poly-L-lactide (PLLA), has shown potential for enhancing bone healing.[3,4] However, current challenges in bone tissue engineering are often related to limited environmental regulation of stem cell attachment, proliferation, and osteogenic differentiation, in particular, the promotion of osteogenic differentiation of cells seeded within three-dimensional (3D) biomaterial scaffolds. The most commonly used approach is the introduction of osteoinductive biofactors, such as bone morphogenetic protein 2 (BMP2).[5] Direct protein delivery is the most developed strategy to introduce bioactive signals into biomaterial-based constructs for tissue repair; however, maintenance of protein stability and bioactivity and the cost and complexity of fabricating a controlled release platform represent some of the current challenges and limitations. Specifically, to achieve therapeutic activity levels, high initial doses, multiple subsequent injections, and variable delivery strategies are often required.

Alternatively, gene therapy methods, such as ex vivo gene transfer of BMP2 to engineer osteogenically enhanced stem cells, have been attempted as a different approach to enhance bone formation.[6] The advantage of gene therapy is the more sustained production of the osteoinductive factor(s); thus, a more generalizable delivery strategy for gene vectors encoding different biofactors may be designed.

Received 24 August 2017; accepted 31 August 2017;
http://dx.doi.org/10.1016/j.omtm.2017.08.008.

[5]Present address: Department of Dermatology, Beijing Tsinghua Changgung Hospital, Tsinghua University, Beijing, 102218, China

[6]Present address: Icahn School of Medicine at Mount Sinai, New York, NY 10029, USA

[7]Present address: Department of Medicine, University of Pittsburgh School of Medicine, Pittsburgh, PA 15219, USA

Correspondence: Bing Wang, MD, PhD, Department of Orthopaedic Surgery, University of Pittsburgh School of Medicine, 450 Technology Drive, Pittsburgh, PA 15219, USA.
E-mail: bingwang@pitt.edu

Correspondence: Rocky S. Tuan, PhD, Center for Cellular and Molecular Engineering, Department of Orthopaedic Surgery, University of Pittsburgh School of Medicine, 450 Technology Drive, Pittsburgh, PA 15219, USA.
E-mail: rst13@pitt.edu

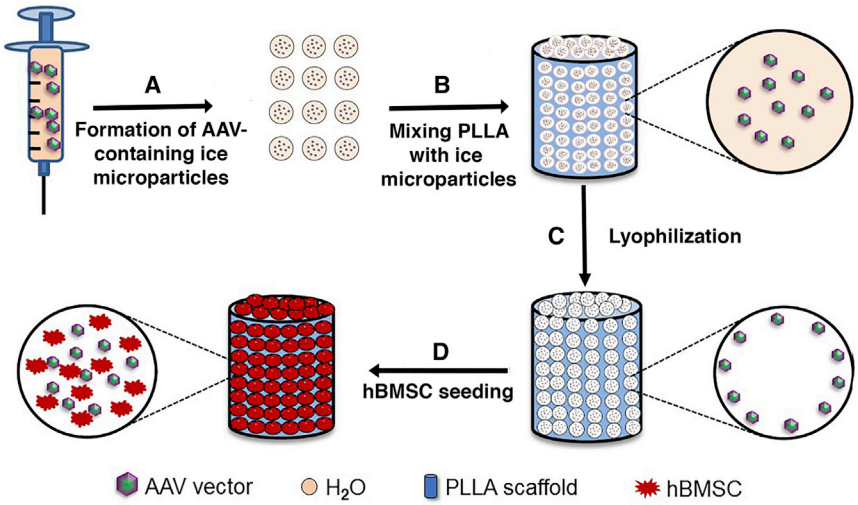

Figure 1. Schematic Representation of the Preparation of AAV-Activated PLLA Scaffold

(A) Concentrated AAV is diluted in PBS and injected through specialized nozzles into liquid nitrogen. Ice microparticles containing AAV are formed, with diameters ranging from 100 to 500 μm. (B) The AAV-containing microparticles are mixed with PLLA solubilized in chloroform (pre-chilled to −20°C). The scaffold is fabricated and porogenized with ice-based microparticles. (C) The porous AAV-PLLA scaffold is formed upon removal of solvent and water by lyophilization, with the ice microparticles acting as the micro-porogen. Enlarged views are provided to represent dispersal of AAV particles onto the walls of the pores within the scaffold upon lyophilization. (D) hBMSCs are seeded into the porous AAV-PLLA scaffold and are subsequently exposed to and infected by the AAV particles released from the interior wall of the pores within the scaffolds, as depicted in the enlarged view of the pores.

However, traditional ex vivo gene therapy is a time-consuming, multi-step process that involves cell culture in vitro,[7] requiring several hours to days prior to introduction in vivo. An alternative approach is to use the biomaterial itself for direct gene delivery, i.e., gene-activated scaffolds,[8] to reduce in vitro preparation time. A key requirement of an optimal gene-activated scaffold is that it needs to not only deliver the appropriate gene, such as the osteoinductive BMP2, but also provide adequate mechanical support. In this manner, stem/progenitor cells will be induced to undergo osteogenesis in a structurally enabling and favorable environment for functional bone formation. Ideally, the biomaterial scaffolds may be used to enhance or control gene transfer relative to traditional delivery methods and promote proliferation and osteogenic differentiation of stem cells by virtue of the more effective, long-term expression of relevant soluble biofactors. This aspect of biomaterial-mediated gene transfer to stem cells encapsulated within a structural scaffold has not been fully explored.

In the last decade, plasmid DNAs have reported successes in matrix-based gene delivery for tissue repair, but their use as a sole agent has been limited by rapid degradation and low gene transfer efficiency.[8] More efficient gene delivery methods, including packaging DNA in either biomaterial particles or with viruses, have been attempted. Indeed, biomaterial-mediated viral vector-based gene transfer, which eliminates prior gene transduction of cells before their encapsulation into scaffolds, has been initiated and has shown promise in overcoming the limitations of growth factor delivery and a traditional ex vivo gene transfection procedure.[9] Given the well-demonstrated benefits of viral vectors, including long-term gene transfer efficiency and improved safety, the combination of gene and cell therapies is being actively explored in both basic and translational research, as well as in clinical trials for bone tissue regeneration.

As a gene transduction vector, recombinant adeno-associated virus (AAV) vector has the distinctly advantageous biological property of being capable of infecting a wide range of host cell types, mediating gene transfer to both dividing and non-dividing cells,[10] and causing low or no immune response,[11] making AAV a particularly desirable vector for musculoskeletal gene therapy. Previous studies have shown enhancement of bone healing by freeze-dry loading AAV2 vectors (RANKL, VEGF, and caALK2) onto allograft[9,12] and AAV2 (BMP2) onto hydroxyapatite (HA).[13] However, the use of a combination 3D biomaterial scaffold incorporated with both stem cells and viral vectors to promote stem cell osteogenesis in situ has not been investigated. In this study, we have explored the use of biomaterial-mediated AAV-vector-based local gene transfer in overcoming the clinical limitations of BMP2 protein delivery and a traditional ex vivo BMP2 gene transfection procedure. The schematic diagram shown in Figure 1 depicts the design and preparation of the ice-based AAV-BMP2 gene-activated PLLA scaffold. The goal of this proof-of-concept study is the assessment of the potential applicability of the ice porogenized scaffold preparation method for the production of biologically active gene-activated PLLA scaffold for hBMSC-based bone formation. Our results demonstrated the efficacy of a BMP2 gene delivery biomaterial consisting of an AAV-based human BMP2 gene-activated PLLA scaffold that was porogenized using ice-based microparticles, resulting in rapid gene expression and osteoinductive effects in naive human bone marrow MSCs (hBMSCs) within the environment of a mechanocompetent biomaterial construct. The in vivo bone formation capacity of this novel gene and cell-activated scaffold were further examined using an intramuscular implantation model in mice. Robust bone formation was observed as early as 4 weeks, with an increase in bone density for up to 10 weeks. These findings strongly suggest the potential of the combination of AAV-based gene transfer with biomaterials for cell-based bone tissue engineering.

RESULTS

Gene-Activated Porous PLLA Scaffold and Cellular Viability of Laden hBMSCs

Ice-based viral microparticles were generated with a median diameter of 250 μm, ranging from 100 to 500 μm (Figures 2A and 2B). After

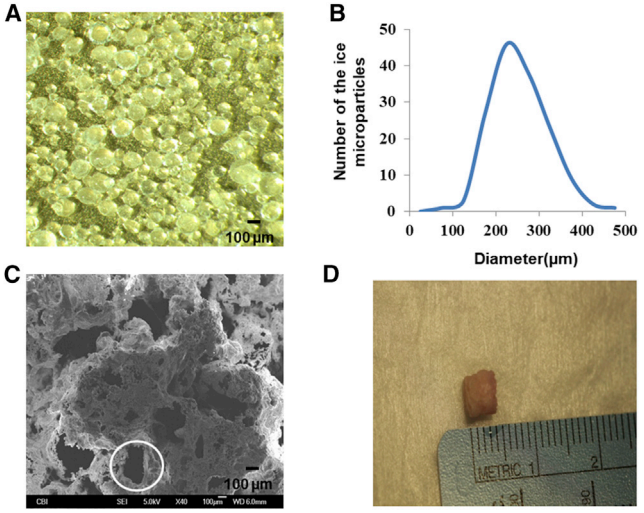

Figure 2. Characterization of Ice-Porogenized PLLA Porous Scaffold

(A and B) Ice microparticles used as a porogen (A), with diameters ranging from 100 to 500 μm (B). Scale bar, 100 μm. (C) SEM image of cross-section of porous PLLA scaffold fabricated using ice-based microparticles (circle indicates pore, with a diameter of around 300–400 μm). Scale bar, 100 μm. (D) Macroscopic view of PLLA porous scaffold fabricated with ice-based microparticles.

freeze drying the mixture of the PLLA solution and ice-based viral microparticles, the spaces occupied by the ice particles were emptied to become pores within the PLLA scaffold. The PLLA, located in the interstitial spaces between the microparticles, became the pore wall of the PLLA scaffolds, and the AAV viral particles nonspecifically remained on the internal surface of the pores. In addition, the contact areas between two adjacent ice-based viral microparticles became small, connecting holes between the adjacent bigger pores, allowing penetration of cells, release and transfer of viral vectors, and passage of nutrients and waste products into and out of the scaffold. As observed by scanning electron microscopy (SEM), the PLLA scaffold containing viral particles appeared to be highly porous, with good pore interconnectivity (Figure 2C). The diameters of pores ranged from 100 to 500 μm, consistent with the size of the virus-containing porogenic ice particles, which satisfy the generally accepted structural requirements for biomaterial scaffold-based bone formation.[14] The PLLA scaffolds were then cut into $4 \times 4 \times 5$ mm^3 blocks for subsequent in vitro and in vivo experiments (Figure 2D).

We examined the biocompatibility of PLLA scaffolds using hBMSCs harvested from human bone marrow, which were also used to test the osteosupportive function of gene-activated PLLA scaffolds. The stem cell characteristics of the hBMSCs were first examined by assay for colony forming unit (CFU) and their capacity to differentiate into multiple mesenchymal lineages, including osteogenesis, adipogenesis, and chondrogenesis (Figure S1). After seeding of hBMSCs into the scaffold, live/dead staining was performed to assess cellular viability. Consistently high cell viability (>85%–90%) was observed, on days 1 and 7 after cell seeding, among the large population of cells encapsulated within the micropore (Figure 3A). As shown in Figure 3B, quantitative results using the MTS colorimetric assay of cell viability also confirmed cell proliferation from day 1 to day 7, with no significant difference between PLLA scaffolds fabricated with or without AAV-BMP2 vector. It should be noted that hBMSC cultures in a 3D biomaterial scaffold, with or without AAV-BMP2 viral particles, showed a consistently lower cell number on days 1 and 7 compared to hBMSC cultures maintained on a two-dimensional (2D) tissue culture plastic (Figure 3B).

Release Kinetics and Activity of AAV Vectors

To determine the most efficient gene delivery vector, we first compared the gene transfer efficiency of AAV2, AAV6, and AAV8 vectors carrying the *GFP* gene in 2D cultured hBMSCs, and found that AAV6-GFP showed the highest level of gene transfer in hBMSCs (Figure S2). We have, therefore, selected AAV6 virus for all subsequent in vitro and in vivo experiments. Because controlled release of viral particles from the gene-activated biomaterial scaffold is critical to the success of gene transduction of the seeded hBMSCs, we determined the release kinetics and functional activity of AAV-GFP released viral particles into the culture medium for up to 20 days. AAV6-GFP virus was chosen for investigation of release kinetics instead of AAV6-BMP2 because the GFP with green fluorescence was able to be detected under microscopy, allowing future calculations of infection efficiency. Because AAV6-BMP2 has the exact same AAV backbone, we believed both AAV vectors should have the same release kinetics. Dot blot assay was used to quantify the viral genome copy number (v.g.) in the daily aliquot of conditioned medium and assess release kinetics of viral vector from the gene-activated scaffold. Results in Figure 4A showed an initial rapid release (11.7% of initial viral load of 5×10^{11} v.g. particles per scaffold), followed by a gradual decrease (0.4% by day 7), thus accounting for a ~35% release of the viral load in the first week. Continuous release was observed for up to 18 days. Interestingly, the second release peak appeared between day 13 and day 16, which might be associated with degradation of the PLLA scaffold. We then calculated the cumulative release over time (Figure 4B), which clearly indicated a fast and major release during days 1–10 and a slow and minor release thereafter. The functional activity of the cumulative released viral particles in media collected at 1, 4, 8, 24, 48, 72, and 96 hr was tested based on gene transduction of hBMSCs. We counted the ratio of GFP^+ cells to determine the infection efficiency of hBMSCs. As shown in Figure S3, GFP^+ cells were observed, indicating the functionality of released AAV. The percentage of GFP^+ hBMSCs increased and plateaued in the medium collected at 96 hr, with a maximal efficiency of around 40%.

AAV-Mediated BMP2 Expression and Osteogenic Differentiation in hBMSCs

We first assessed the efficacy of AAV-mediated BMP2 expression in hBMSCs ELISA. Results obtained on 2-week cultures of hBMSCs with or without AAV-BMP2 infection and seeded on tissue culture plastic demonstrated AAV-mediated BMP2 expression (Figure 5A). Interestingly, there was no significant difference ($p > 0.05$) between BMP2 expression levels in 2D cultured and PLLA 3D cultured

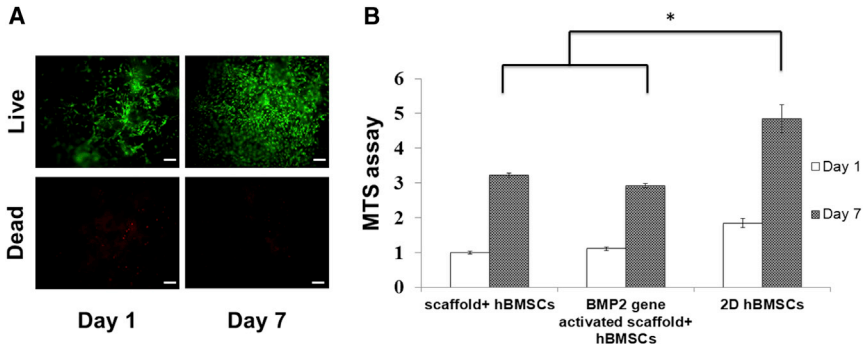

Figure 3. Cell Viability of hBMSCs Laden on AAV-Activated Porous PLLA Scaffolds

(A) Live/dead staining of cells seeded within AAV-activated scaffold surface 1 day (left) and 7 days (right) after seeding. Scale bar, 100 μm. (B) CellTiter 96 AQueous One Solution Cell Proliferation Assay (MTS) analysis of metabolic activity of hBMSCs seeded in PLLA scaffolds fabricated with or without AAV-BMP2 viral constructs and on two-dimensional plates at culture days 1 and 7. All data were normalized to data from hBMSCs cultures on plain PLLA scaffolds (fabricated without AAV-BMP2 constructs) on day 1.

hBMSCs infected at the same MOI of 1×10^6 v.g. For 3D cultures in PLLA scaffolds, we also detected BMP2 expression levels 2 weeks after culture, including those consisting of hBMSCs infected with AAV-BMP2 (1.6×10^5 cells) prior to seeding (pre-transduced), naive hBMSCs (1.6×10^5 cells) seeded with AAV-BMP2 (5×10^{11} v.g. of particles) (co-transduced), and naive hBMSCs (1.6×10^5 cells) seeded with BMP2 protein (1 μg) (protein only). We found that BMP2 expression was elevated in the above three groups as compared to the control group that was fabricated with naive hBMSCs alone ($p < 0.001$, $p < 0.001$, and $p < 0.05$, respectively). In a further analysis, we found that both the pre-transduced and co-transduced constructs exhibited significantly higher BMP2 levels compared to the protein-only constructs ($p < 0.01$ and $p < 0.01$). Interestingly, we also found that the pre-transduced cultures (MOI, 1×10^6 v.g.) showed a higher level of BMP2 protein in the medium compared to the co-transduced cultures seeded within the gene-activated scaffold (MOI, 3×10^6 v.g.), despite the latter starting with a higher MOI. This difference could be attributed to the retention of some of the viral particles loaded within that scaffold at 2 weeks that might not have been available or accessible for hBMSC infection.

We next assessed the extent of osteogenesis in the hBMSC cultures by means of qRT-PCR analysis of osteoclacin (OCN) and bone sialoprotein (BSP2) gene expression after 6 weeks of culture. As shown in Figures 5B and 5C, no significant difference was seen between 2D and 3D cultures of AAV-BMP2-transduced hBMSCs. In 3D PLLA constructs, gene expression levels of OCN and BSPII were higher in AAV-BMP2 pre-transduced cultures compared to the co-transduced cultures ($p < 0.05$ and $p < 0.05$, respectively). However, both groups had remarkably higher levels of OCN and BSPII expression compared to the protein-only group ($p < 0.01$, $p < 0.01$). Although BMP2 gene expression was evident in the BMP2 protein only PLLA cultures at 2 weeks, no increase in the expression of other osteogenesis-related genes, including OCN and BSP2, was detected at 6 weeks. Whether this resulted from the degradation or loss of BMP2 from the culture medium is unknown.

Bone Formation Functionality of AAV-BMP2 Gene-Activated Constructs In Vivo

The in vivo osteogenic functionality of the gene-activated scaffold was tested by implantation of three experimental hBMSC-loaded PLLA constructs into the thigh muscles of SCID mice, including (1) AAV-BMP2 activated scaffolds (5×10^{11} v.g. of particles); (2) AAV-GFP activated scaffolds (5×10^{11} v.g. of particles); (3) BMP2 protein laden scaffolds (1 μg); and (4) scaffold-only controls. All implanted scaffolds were seeded with 1.6×10^5 hBMSCs, and each group consisted of 4 mice (8 samples per group). The presence of mineralized bone was determined by micro-computed tomography (CT) imaging at 4 weeks. As shown in Figure 6A, at week 4, PLLA scaffold activated by embedded AAV-BMP2 viral particles was able to support gene transduction of hBMSCs in situ to enhance their osteogenic differentiation, resulting in improved intramuscular bone formation compared to AAV-GFP-activated scaffolds, BMP2 protein laden scaffolds, and the scaffold-only control, with the latter showing no detectable bone formation. Because double-strand AAV-mediated gene expression generally starts at week 3 and reaches plateau at 5 to 6 weeks after administration in vivo,[15] we postulated that the neo-bone tissue should become denser and more calcified following the above time course of BMP2 expression. Therefore, ectopic bone formation was examined at 4, 6, 8, and 10 weeks using micro-CT. The results showed a significant increase in bone size during weeks 6–10, matching the temporal profile of BMP2 transgene expression (Figure 6B). Further analysis showed a positive correlation between time and bone density: 293.5 ± 21.2 (week 4), 352.2 ± 6.7 (week 6), 407.3 ± 8.2 (week 8), and 435.9 ± 16.6 mg (week 10) HA/cm^3 (Figure 6C). The 10-week post-implantation specimen was then analyzed for calcium content (Figure 7). The AAV-BMP2 gene-activated constructs were found to have a significantly higher level of calcium (23.4 ± 1.1 mg/construct) than BMP2-protein-loaded constructs (15.3 ± 2.8 mg/construct) and naive-hBMSC-loaded constructs (13.8 ± 1.3 mg/construct) ($p < 0.01$, $p < 0.001$). However, there was no significant difference between BMP2-loaded PLLA constructs and PLLA-alone constructs at 10 weeks post-implantation ($p > 0.05$). These results agreed with the micro-CT imaging data in Figure 6 that the high calcium density of the construct in the AAV-BMP2-gene-activated constructs met with the requirement of ectopic, intramuscular bone formation, but the BMP2-protein-loaded constructs did not. The nature of the neo-bone formation was further examined histologically. As shown in Figure 8, H&E and Herovici staining demonstrated the existence of ectopic bone formation in the AAV-BMP2-activated PLLA scaffold seeded with hBMSCs, in which we found the formation of bone matrix consisting of collagen fibers in

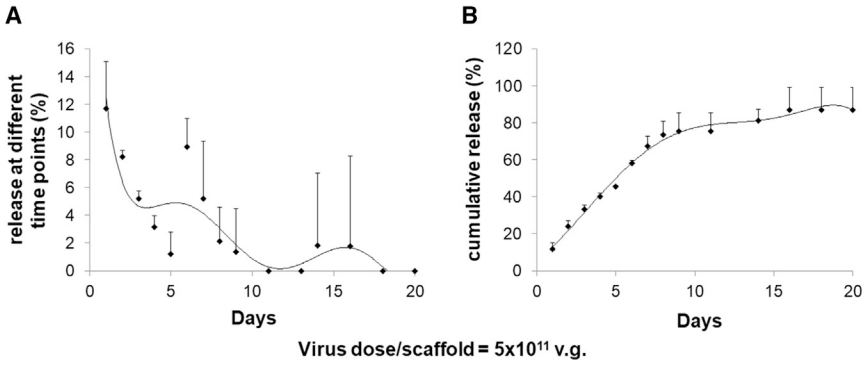

Figure 4. Release Kinetics of AAV Particles from Gene-Activated Porous PLLA Scaffolds

(A) Dot blot quantification of daily release of AAV-GFP v.g. of particles in incubation medium up to day 20 (initial load = 5 × 10^{11} v.g. of particles per scaffold). (B) The cumulative release over time clearly indicated fast and major release from day 1 to 10 and subsequent slow and minor release. n = 3.

the muscle (black arrows, bottom). However, no ectopic bone formation was seen in the PLLA-based implants consisting of either hBMSCs loaded with BMP2 protein or naive hBMSCs alone, as demonstrated by porous-only structures with no signs of calcification.

To investigate the origin of ectopic bone formation, i.e., from donor cells (human MSCs within the scaffold) or endogenous cells (mouse host cells), we performed human nuclear antigen immunohistochemistry analysis to distinguish human cells from mouse cells. We observed negative staining in the newly formed bone tissues, suggesting the absence of human cells (Figure S4). It should be noted that we did not perform time-course tracking of hBMSCs over the 6 weeks; thus, further investigation is needed to ascertain whether hBMSCs are capable of differentiating into bone cells at earlier time points but are cleared at the late stage by host cells or whether they do not differentiate into bone cells during the entire bone formation process.

DISCUSSION

Ideal bone tissue engineering scaffolds should not only mimic local tissue architecture, for example, the physical and structural variation in different bones and defects, but also support robust osteogenic differentiation of cells seeded within the 3D scaffold, which requires the sustained introduction of osteoinductive biofactors, such as BMP2. BMP2, known to be important for bone development and healing, has been applied successfully for bone therapy;[16] however, pitfalls, such as risk of carcinogenicity of recombinant human BMP2 (rhBMP2), are associated with the dose, carrier, and delivery approach.[17] Therefore, one promising approach is to develop a biomimetic scaffold material, used for stem cell seeding, that is also capable of controllably delivering gene transduction vectors in situ to drive the expression of osteoinductive gene(s) for genetic engineering of the seeded or host cells. There are two main types of vectors for gene transfer in the context of gene-activated matrices, i.e., plasmid DNA and viral vectors. Although induction of osteogenic or chondrogenic differentiation via non-viral gene-activated materials has been attempted for MSC-based tissue engineering of bone and cartilage,[18] biomaterial-mediated osteoinductive gene transfer to stem cells using AAV vectors has not been fully explored.

The properties of the scaffolds generated in this study satisfy a number of specific criteria: (1) the scaffolds are highly porous, with an interconnected pore network and appropriate pore size to facilitate cell migration, viral vector release, and bone formation; (2) the scaffold's biomaterial, PLLA, is biocompatible and mechanically similar to native bone; and (3) the scaffold fabrication method is efficient and non-destructive to viral vectors. Among the currently available synthetic, biodegradable biomaterials, we selected PLLA because of its well-known biocompatibility and its biodegradation characteristics create a favorable microenvironment to promote biochemically, structurally, and mechanically matched natural bone healing.[19] In studies performed both in our laboratories and by others, tissue engineering using hMSCs on a porous PLLA scaffold has shown the potential for enhancing bone healing.[3,4] In particular, we have recently developed a novel fabrication method for a porous PLLA scaffold using ice-based micro-porogens to produce a 3D platform that supports improved cell interaction with the polymeric scaffold and presents a biocompatible physical and chemical environment.[20] Therefore, in this study, we have fabricated gene-activated porous PLLA scaffolds using the ice-based microparticle porogenization method. Because ice can be easily sublimed by freeze drying, without the use of additional organic solvents for porogen leaching and fabrication of porous scaffolds, this procedure represents a new candidate technology for the efficient delivery of matrix-based viral vector for tissue repair.[20,21]

At present, the use of single-step and imaging-guided fabrication of a biomaterial scaffold incorporated with both stem cells and viral vectors to promote bone repair in vivo has not been fully investigated. In the technology described here, as schematized in Figure 1, ice-based microparticles function both as the porous micro-porogen and as a vehicle to generate in the biomaterial scaffold a 3D porous environment with the correct pore size to support bone formation and provide good pore interconnectivity for nutrient perfusion as well as provide support for cell attachment, proliferation, and differentiation. Data from the MTS assay (Figure 3B) show that the hBMSCs continue to proliferate after being seeded onto the 3D porous PLLA scaffold, although they are less metabolically active compared to those in 2D culture. During the one-step ice-based fabrication of the PLLA scaffold, viral particles are embedded in ice and are not exposed to harsh organic solvents and may be released at a controllable rate to infect seeded hBMSCs (Figure 1). Our results

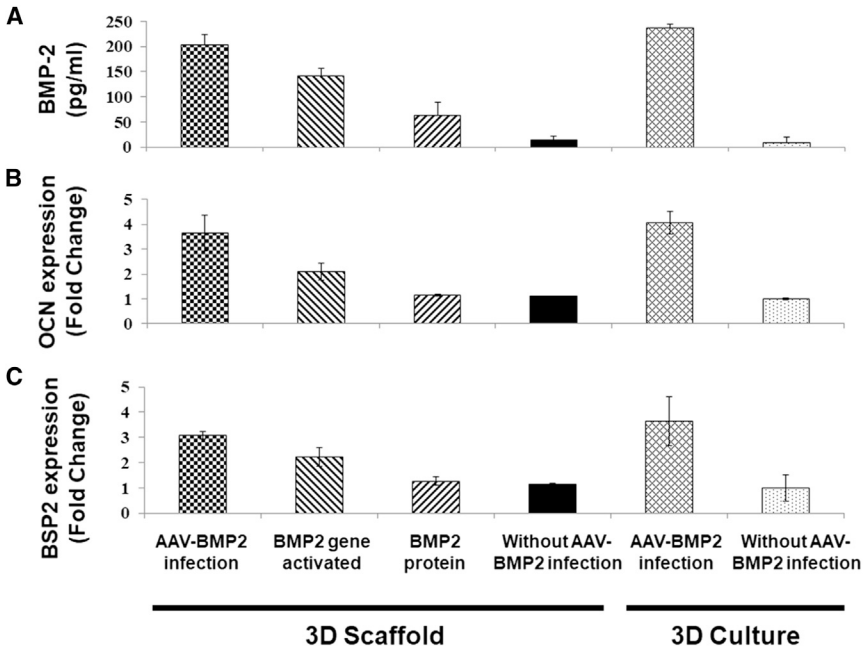

Figure 5. Effect of Various 2D and 3D Culture Conditions on BMP2 and Osteogenic Gene Expression by hBMSCs after 2 Weeks of Culture

(A) BMP2 level (pg/mL) determined by ELISA. (B and C) Relative gene expression of OCN (B) and BSP2 (C) by qRT-PCR. Data for fold change of gene expression are normalized to those of 2D hBMSC cultures without BMP2 infection.

show that the BMP2 gene-activated PLLA scaffold, based on cellular viability, has high efficiency as a viral vector delivery platform during the entire fabrication process, without any sign of viral toxicity. On the basis of these characteristics, we have developed here a single-step protocol using the ice porogen-based technology[20] to deposit AAV vectors into a porous PLLA scaffold. Our results show that functional AAV vectors can be successfully transferred onto the pore wall of PLLA porous scaffolds.

Currently, the use of AAV-based gene constructs has emerged as a promising gene delivery vehicle, considering its broad cell tropism and lack of an inflammatory response.[22] Gene delivery by AAV vectors persists mainly in episomal or concatameric form but does not involve integration into host chromosomal DNA,[23] which reduces the risk of BMP2-associated carcinogenicity compared to the high dose and long-time use of rhBMP2 in spine surgery. Different serotypes of AAV vectors share a similar structure, size, and genetic organization and only significantly differ in amino acid composition of the capsid proteins, which dictate receptor specificity.[24] Here, we found that AAV6 has higher efficacy for hBMSCs (Figure S2) compared to AAV2 and AAV8. Previous studies have shown the potential of AAV as a viral vector for bone healing through ex vivo gene transfer of BMP2[7] and direct injection of the AAV-BMP2 vector in vivo,[11] but little attention has been paid to more controlled gene delivery using 3D matrices. Our one-step fabrication method enables the direct, non-specific deposition of AAV vectors onto the porous scaffold wall, representing a simple and efficient method of matrix-based gene delivery. The viral-vector release rate within the scaffold is controlled by scaffold degradation, fluid exchange through the scaffold, and cell infiltration. Moreover, by varying the AAV viral particle concentration in the ice-based micro-porogens, the virus load per micropore may be precisely controlled. In our in vitro viral vector release kinetics test, a scaffold carrying 5×10^{11} v.g. of particles maintained effective release of functional AAV vector for 1 week, as demonstrated by dot blot analysis showing that only 35% of total viral particles were released to the outside of the scaffold before PLLA biodegradation, thus indicating that the majority of the virus load was adequately maintained within the scaffold for long-term infection of seeded hBMSCs. This was confirmed by our finding of efficient BMP2 expression in constructs cultured in vitro and ectopic bone formation in vivo upon implantation of the construct in the hindlimb muscle of SCID mice.

As shown in Figure 5A, we observed a high BMP2 level in the gene-activated group after 14 days, suggesting a continuous production of BMP2 from cells, which agrees with the results from our recently published study.[25] In that relevant study using the same strategy but different material, we found the peak of transduction efficiency (from 70% to 82%) on day 7. At day 14, there was still a considerable number of transduced cells.

We also noticed that at day 14, BMP2 level in the medium from BMP2 protein group was very low, indicating the complete release of BMP2 from scaffolds. In addition, we did not observe bone formation in the BMP2 protein loading group in vivo. The dose we chose (1 μg of BMP2) should cause bone formation in vivo.[26–31] To further understand the mechanism causing no bone formation in this group, we performed a BMP2 release experiment from PLLA. We loaded 1 μg of BMP2 into a scaffold, incubated it in PBS, and collected the solution at a different time point. Afterward, the BMP2 amount was quantitated using ELISA. As shown in Figure S5, we found that most of the protein was released on the first 3 days. We believe rapid release of BMP2 protein from highly porous PLLA scaffolds caused significantly lower osteogenic gene expression (Figures 5B and 5C) and no bone formation (Figures 6 and 7) in this group.

We suggest that the technology reported here and schematized in Figure 1 provides a universal delivery strategy for the delivery of any gene therapeutic constructs, viral, plasmid, or other nucleic

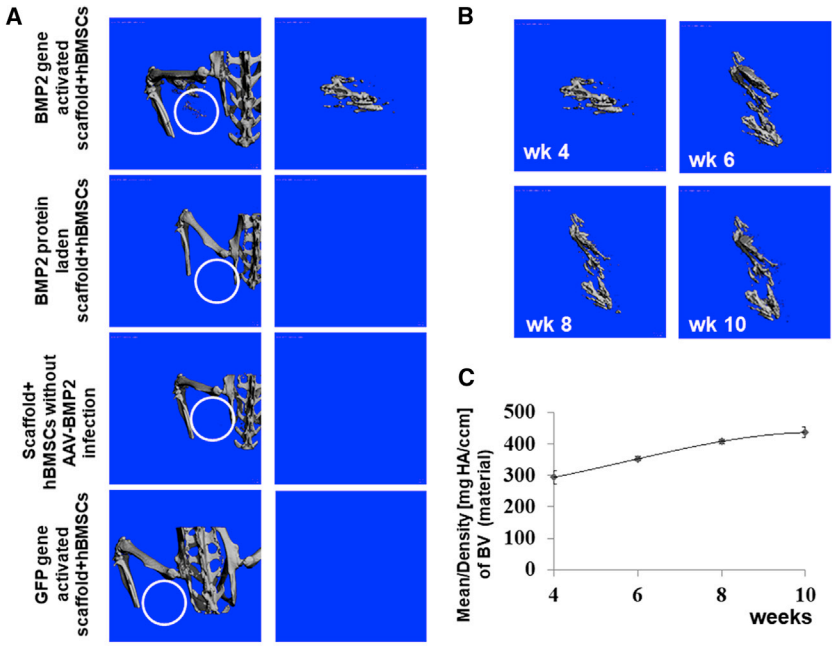

Figure 6. Bone Formation In Vivo after Implantation of hBMSC-Seeded AAV-BMP2 Gene-Activated Constructs

Four groups of hBMSC-seeded PLLA scaffolds were used: (1) AAV-BMP2 activated; (2) AAV-GFP activated; (3) laden with BMP2 protein; and (4) control. (A) Micro-CT detection of ectopic bone formation at 4 weeks post-implantation. Bone formation was detected in the implantation site (circles) of an AAV-BMP2-activated scaffold seeded with hBMSCs, but not in similar areas with an AAV-GFP-activated or BMP2 protein laden scaffold or in a scaffold seeded only with hBMSCs. (B and C) Three-dimensional micro-CT reconstruction (B) and mean density (C) of ectopic neo-bone tissue formation in hBMSC-seeded AAV gene-activated PLLA constructs as a function of time after implantation.

acid complexes, for a variety of tissue engineering applications. To enhance activities of the cells seeded within the gene-activated scaffold, future variations may include (1) design of bio-responsive scaffold biomaterials, e.g., those that degrade upon exposure to cell-released enzymes, such as proteases; and (2) activation of the inner surface of the micropores by adding bioactive proteins (e.g., extracellular matrix components) or growth factor ligands into the ice-based microparticles to enhance cell migration and proliferation within the scaffold.[8]

Our findings demonstrate that the ice-based porogenized scaffolds described here are well-suited for the repair of a simple and uncomplicated bone defect and is potentially clinically applicable, involving only a single-step fabrication method to produce an MSC-loaded, osteogenesis-promoting construct for bone formation.

MATERIALS AND METHODS

hBMSC Isolation and Characterization

hBMSCs were isolated with Institutional Review Board approval (University of Washington and University of Pittsburgh) from femoral heads of a 58-year-old female undergoing total hip arthroplasty using a standard plastic adhesion protocol. hBMSCs were then cultured in growth medium (minimum essential medium eagle - alpha modification [α-MEM] + 10% MSC qualified fetal bovine serum [FBS] [all Gibco/Life Technologies, Grand Island, NY] + 1 ng/mL fibroblast growth factor 2 [FGF-2] [R&D Systems, Minneapolis, MN] + antibiotic-antimycotic), seeded into T150 flasks (Corning, Tewksbury, MA), and incubated at 37°C with 5% CO_2. At 80% confluence, adherent cells were detached with 0.25% trypsin in 1 mM EDTA (Invitrogen, Carlsbad, CA) and passaged. The stem cell characteristics of the hBMSCs were examined by standard CFU assay and tri-lineage differentiation potential upon culturing in appropriate, specific differentiation induction medium by Alizarin Red staining (osteogenesis), Oil Red O staining (adipogenesis), and Alcian Blue staining (chondrogenesis).[32] For all studies, passage 5 hBMSCs were used.

Construction and Production of AAV Vectors

The full-length cDNAs of human BMP2 (1.2 kb) and the GFP reporter were cloned into double-stranded AAV vectors (dsAAVs)[7,15] under the control of the CMV promoter, respectively. Serotypes 2, 6, and 8 of AAV vectors were purified twice with CsCl gradient ultracentrifugation according to our previously published protocol.[33] As we reported previously,[34] the titers of v.g. of particles were determined by a standard dot blot, yielding approximately 0.5 × 1013 to 1.0 × 1013 v.g. of viral particles per mL. Because each dsAAV particle has two viral genomes, actual AAV particle titers are only half of the v.g. number detected in the dot blot assay. To test gene transfer efficiency of different serotypes of AAV vectors in hBMSCs, cells in the 6-well plate at 70% confluence were infected with serotypes 2, 6, and 8 rAAV-CMV-GFP vectors at MOI of 1 × 104 v.g. and transduction efficiency was determined by under the fluorescence microscopy 48 hr post-infection.

Preparation of Ice-Encapsulated Viral Microparticles

AAV viral particles were first diluted to the desired concentration in PBS. Ice-based viral microparticles were then generated by injecting AAV vector solution through specialized nozzles (0.5 μm tip I.D. pre-pulled pipets, World Precision Instruments, Cat. No. TIPO5TW1F-L, Sarasota, FL) powered via syringe pump (Harvard Apparatus, Holliston, MA) into liquid nitrogen. The optimal distance between the nozzles and liquid nitrogen was 3.5 in to obtain microparticles with diameters ranging from 100 to 500 μm, as observed using a microscope (Olympus SZX16, Waltham, MA) and size analyzed using NIH ImageJ, which were desirable for bone tissue engineering.[14]

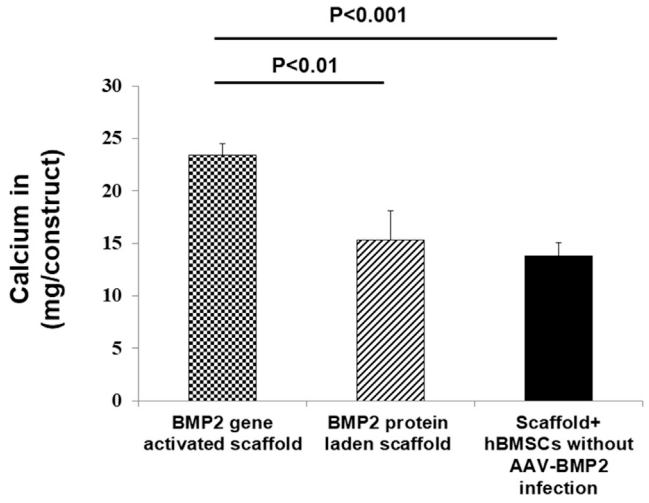

Figure 7. Quantification of Calcium Accumulation in hBMSC-Seeded PLLA Scaffold-Based Implants at 10 Weeks Post-implantation

Three groups of PLLA scaffolds were used: (1) AAV-BMP2 activated; (2) laden with BMP2 protein; and (3) control. Gene-activated scaffold-based constructs showed a statistically higher level of calcium accumulation.

Fabrication of Gene-Activated Scaffolds

PLLA (molecular weight = 85–160 kD), purchased from Sigma Aldrich (St. Louis, MO), was dissolved (10% by weight) in chloroform and cooled to −20°C overnight. PLLA solution (0.5 mL) and ice-encapsulated viral microparticles (1 mL) were mixed evenly in a pre-chilled (20°C) stainless steel container and shaped by pre-chilled stainless steel molds on dry ice. Finally, the 4 × 4 × 5 mm^3 scaffold samples, each containing 5 × 10^{11} v.g. of AAV particles, were kept in liquid nitrogen overnight and freeze dried in the lyophilizer for 4 hr to completely remove the solvent and water to produce the 3D gene-activated porous polymeric scaffolds. To examine the interior ultrastructure of the scaffolds, samples without AAV vectors were bisected and immediately lyophilized, and the cross-section was imaged by SEM using the JEOL JSM6335F SEM, which was operated at 3 kV accelerating voltage and 8 mm working distance in the University of Pittsburgh Center for Biological Imaging.

Cell Viability

After the scaffolds were sterilized with 70% ethanol for 10 min, lyophilized, and rinsed with DMEM (Gibco/Life Technologies), they were seeded evenly and slowly with 20 μL of hBMSC cell suspension (about 1.6 × 10^5 cells). The cell-seeded, AAV-loaded scaffolds were placed individually into a 48-well plate and maintained in an incubator at 37°C and 5% CO_2 for 4 hr to allow cell adhesion to the scaffolds, and then DMEM (500 μL) was added for overnight viral infection. 500 μL of complete medium (DMEM+ 1x antibiotic-antimycotic + 20% MSC qualified FBS [all Gibco/Life Technologies]) was added on day 2. Cell viability was assessed via calcein acetoxymethyl ester (calcein-AM) and ethidium homodimer-1 (EthD-1) staining (live/dead kit, Invitrogen) after 24 hr and 7 days. Cell proliferation ability was quantified by MTS assay (CellTiter 96 Aqueous Cell Proliferation assay, Promega, Madison, WI) on day 1 and 7.

AAV Vector Release Kinetics

AAV gene-activated scaffolds prepared using the fabrication method described above were ethanol-sterilized, rinsed in DMEM, and then incubated in 100 μL of DMEM. An aliquot of the incubating medium was collected at different time points lasting for 20 days and analyzed for release of the viral particles from the scaffold with a dot blot hybridization assay using a CMV promoter probe.[33,34] Standardization of the dot blot was done using known AAV viral titers, and release kinetics of AAV viral particles from the scaffold were determined. The functional activity of the cumulative, released AAV particles in media collected at 1, 4, 8, 24, 48, 72, and 96 hr was tested based on gene transduction of hBMSCs. hBMSCs were cultured to ~70% confluence in 24-well plates and infected with the conditioned medium collected at 1, 4, 8, 24, 48, 72, and 96 hr, and the percentage of positive cells observed was based on the expression level of GFP (% microscopically GFP^+ cells).

Protein and Gene Expression Analyses

To confirm in vitro functionality of AAV-activated porous PLLA scaffolds, the supernatant of the hBMSC-seeded, gene-activated constructs after 2 weeks of culture was processed for BMP2 ELISA assay and carried out according to the manufacturer's protocol (R&D Systems, Minneapolis, MN). We also tested the BMP2 protein release profile from the BMP2-loaded scaffold. Briefly, 1 μg of BMP2 protein (PeproTech, Rocky Hill, NJ) was loaded into scaffolds and then soaked into PBS for up to 14 days in a cell culture incubator, with medium changes every 2 days. BMP2 released into PBS at different points was measured by ELISA using the same method described above. Gene expression in the constructs after 6 weeks of culture was also carried out using RNA extracted from the samples using an RNeasy plus mini kit (QIAGEN Sciences, Valencia, CA). Reverse transcription-PCR was performed using SYBR Green PCR master mix (Applied Biosystems, Foster City, CA) on a 7900HT Fast Real-Time PCR machine (Applied Biosystems) under the following conditions: 94°C for 5 min, 40 cycles of 94°C for 30 s, 60°C for 30 s, 72°C for 30 s, and 72°C for 5 min. The transcription level of GADPH was used as endogenous control. The transcript levels of OCN and BSP2 were analyzed using gene-specific primers and the comparative CT (ΔΔCT) method according to our published protocol.[35]

Animal Experiment

All experimental procedures were approved by the Institutional Animal Care and Use Committee of the University of Pittsburgh. 20-μL suspensions of hBMSCs (~1.6 × 10^5 cells) were seeded into gene-activated porous PLLA scaffolds that were fabricated as described above. The cell-seeded constructs were maintained in an incubator at 37°C and 5% CO_2 for 4 hr to allow cell adhesion, and then DMEM (500 μL) was added and the cultures were maintained for an additional 12 hr for viral infection. As shown in Figure 2D,

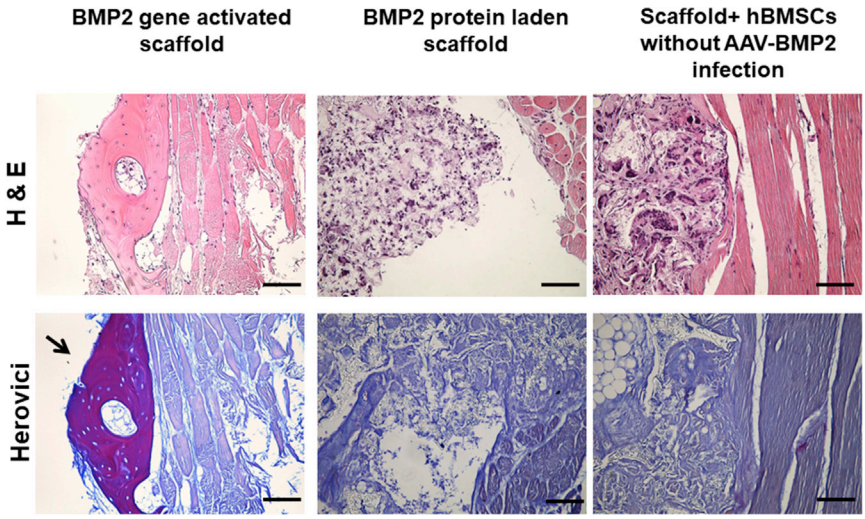

Figure 8. Histological Analysis of hBMSC-Seeded PLLA Scaffold-Based Implants at 10 Weeks Post-implantation by H&E (Top Row) and Herovici Staining (Bottom Row)

Three groups of PLLA scaffolds were used: (1) AAV-BMP2 activated; (2) laden with BMP2 protein; and (3) control. Robust ectopic neo-bone formation is seen in the AAV-BMP2 gene-activated scaffold group. Scale bar, 100 μm.

the constructs (scaffold size: $4 \times 4 \times 5$ mm^3) were implanted in the hindlimbs (thigh muscles) of 2-month-old SCID mice (NOD.CB17 PRKDA SCID/J, Jackson Laboratory, Bar Harbor, ME) using our previously published protocol.[7] Bilateral implantation was performed after the mice were anesthetized with 2% to 3% isoflurane and maintained in a surgical plane during the procedure with 1.5% isoflurane. Three groups of 4 mice (8 samples in each group) each were used as required by power analysis, and the implants consisted of (1) AAV6-BMP2 scaffold (dose: 5×10^{11} v.g. particles) + hBMSCs (1.6×10^5 per scaffold); (2) BMP2 protein scaffold (each scaffold loaded with 1 μg of BMP2 protein; PeproTech, Rocky Hill, NJ) + hBMSCs (1.6×10^5 per scaffold); (3) scaffold only + hBMSCs (1.6×10^5 per scaffold); and (4) AAV-GFP scaffold (dose: 5 × 1011 v.g. particles) + MSCs (1.6×10^5 per scaffold).

Micro-CT Analyses

Ectopic bone formation was vitally monitored with micro-CT (vivaCT 40, Scanco Medical, Switzerland). After obtaining two-dimensional image slices from the micro-CT, the view of interest (VOI) was uniformly delineated. 3D reconstructions were created using an appropriate threshold that was kept constant throughout the analyses. The bone morphometric and density measurements followed the guidelines set by the American Society of Bone and Mineral Research.[36]

Calcium Quantification and Histological Analyses

The hindlimb muscle and scaffold construct of the SCID mice were taken out 10 weeks after implantation. The samples were cut in half, with one half pulverized and extracted for 3 days in 1 mL of 1 N HCl in a 1.5 mL microcentrifuge tube. The calcium concentration in the supernatant was measured using a Calcium Colorimetric Assay Kit (Abnova, Taiwan). The remaining half of the samples was fixed in 4% paraformaldehyde for 3 days, decalcified in 10% EDTA for 3 weeks, dehydrated and embedded in paraffin, and sectioned at 5 μm thicknesses. Sections were histologically stained with H&E and Herovici stain to visualize general tissue morphology and collagen type I positive bone matrix formation. All sections were examined under bright-field microscopy.

Immunohistochemistry

Briefly, histological sections were subjected to antigen retrieval and peroxidase blocking in 3% H_2O_2 and further blocked in horse serum. Primary antibody (rabbit anti-human Ku80; Cell Signaling Technology, Danvers, MA) was applied and incubated overnight at 4°C. Detection of primary antibody was performed with biotinylated goat anti-rabbit antibodies (Vector Labs). Secondary peroxidase-conjugated antibodies were visualized using a Vectorstain Elite ABC and developed with the VIP kit (Vector Labs). Images were captured with a CKX41 microscope (Olympus, Japan) equipped with a Leica DFC 3200 camera.

Data Collections and Statistics

All data shown are mean ± standard error. Statistical significance between two measurements was evaluated by unpaired Student's t test, with significance set at $p < 0.05$. All in vitro experiments were performed in triplicates.

SUPPLEMENTAL INFORMATION

Supplemental Information includes five figures and can be found with this article online at http://dx.doi.org/10.1016/j.omtm.2017.08.008.

AUTHOR CONTRIBUTIONS

J.X. performed the PLLA scaffold, BMP2 ELISA, ALP staining, real-time PCR, and immunohistochemistry and wrote the manuscript. H.L. performed tests for stem cell differentiation, function analysis of viral vectors and BMP2 protein from scaffolds and additional experiments for revision. A.B. prepared the PLLA scaffold and conducted BMP2 release. Y.T. prepared the vectors, participated in animal surgery and care, and analyzed the micro-CT imaging. J.T. provided stem cells and identified stem cells. Design and supervision of the study, data interpretation, and writing and correction of the manuscript were performed by R.S.T. and B.W.

CONFLICTS OF INTEREST

The authors declare no competing financial interests.

ACKNOWLEDGMENTS

This study was funded in part by the Pennsylvania Commonwealth Department of Health (SAP4100061184) and supported by the China Scholarship Council (Tsinghua University).

REFERENCES

1. Peng, H., Wright, V., Usas, A., Gearhart, B., Shen, H.C., Cummins, J., and Huard, J. (2002). Synergistic enhancement of bone formation and healing by stem cell-expressed VEGF and bone morphogenetic protein-4. J. Clin. Invest. *110*, 751–759.
2. Damien, C.J., and Parsons, J.R. (1991). Bone graft and bone graft substitutes: a review of current technology and applications. J. Appl. Biomater. *2*, 187–208.
3. Stylios, G., Wan, T., and Giannoudis, P. (2007). Present status and future potential of enhancing bone healing using nanotechnology. Injury *38* (*Suppl 1*), S63–S74.
4. Tuli, R., Nandi, S., Li, W.J., Tuli, S., Huang, X., Manner, P.A., Laquerriere, P., Nöth, U., Hall, D.J., and Tuan, R.S. (2004). Human mesenchymal progenitor cell-based tissue engineering of a single-unit osteochondral construct. Tissue Eng. *10*, 1169–1179.
5. Edgar, C.M., Chakravarthy, V., Barnes, G., Kakar, S., Gerstenfeld, L.C., and Einhorn, T.A. (2007). Autogenous regulation of a network of bone morphogenetic proteins (BMPs) mediates the osteogenic differentiation in murine marrow stromal cells. Bone *40*, 1389–1398.
6. Kumar, S., Nagy, T.R., and Ponnazhagan, S. (2010). Therapeutic potential of genetically modified adult stem cells for osteopenia. Gene Ther. *17*, 105–116.
7. Mi, M.Y., Tang, Y., Salay, M.N., Li, G., Huard, J., Hu, F.H., Niyibizi, C., and Wang, B. (2009). AAV based *ex vivo* gene therapy in rabbit adipose-derived mesenchymal stem/progenitor cells for osteogenesis. Open Stem Cell J. *1*, 69–75.
8. Cam, C., and Segura, T. (2013). Matrix-based gene delivery for tissue repair. Curr. Opin. Biotechnol. *24*, 855–863.
9. Ito, H., Koefoed, M., Tiyapatanaputi, P., Gromov, K., Goater, J.J., Carmouche, J., Zhang, X., Rubery, P.T., Rabinowitz, J., Samulski, R.J., et al. (2005). Remodeling of cortical bone allografts mediated by adherent rAAV-RANKL and VEGF gene therapy. Nat. Med. *11*, 291–297.
10. Rabinowitz, J.E., and Samulski, J. (1998). Adeno-associated virus expression systems for gene transfer. Curr. Opin. Biotechnol. *9*, 470–475.
11. Chen, Y., Luk, K.D., Cheung, K.M., Xu, R., Lin, M.C., Lu, W.W., Leong, J.C., and Kung, H.F. (2003). Gene therapy for new bone formation using adeno-associated viral bone morphogenetic protein-2 vectors. Gene Ther. *10*, 1345–1353.
12. Koefoed, M., Ito, H., Gromov, K., Reynolds, D.G., Awad, H.A., Rubery, P.T., Ulrich-Vinther, M., Soballe, K., Guldberg, R.E., Lin, A.S., et al. (2005). Biological effects of rAAV-caAlk2 coating on structural allograft healing. Mol. Ther. *12*, 212–218.
13. Nasu, T., Ito, H., Tsutsumi, R., Kitaori, T., Takemoto, M., Schwarz, E.M., and Nakamura, T. (2009). Biological activation of bone-related biomaterials by recombinant adeno-associated virus vector. J. Orthop. Res. *27*, 1162–1168.
14. Loh, Q.L., and Choong, C. (2013). Three-dimensional scaffolds for tissue engineering applications: role of porosity and pore size. Tissue Eng. Part B Rev. *19*, 485–502.
15. Wang, Z., Ma, H.I., Li, J., Sun, L., Zhang, J., and Xiao, X. (2003). Rapid and highly efficient transduction by double-stranded adeno-associated virus vectors in vitro and in vivo. Gene Ther. *10*, 2105–2111.
16. Poon, B., Kha, T., Tran, S., and Dass, C.R. (2016). Bone morphogenetic protein-2 and bone therapy: successes and pitfalls. J. Pharm. Pharmacol. *68*, 139–147.
17. Skovrlj, B., Koehler, S.M., Anderson, P.A., Qureshi, S.A., Hecht, A.C., Iatridis, J.C., and Cho, S.K. (2015). Association between BMP-2 and carcinogenicity. Spine *40*, 1862–1871.
18. Raisin, S., Belamie, E., and Morille, M. (2016). Non-viral gene activated matrices for mesenchymal stem cells based tissue engineering of bone and cartilage. Biomaterials *104*, 223–237.
19. Kanczler, J.M., and Oreffo, R.O. (2008). Osteogenesis and angiogenesis: the potential for engineering bone. Eur. Cell. Mater. *15*, 100–114.
20. Li, J., Chen, Y., Mak, A.F., Tuan, R.S., Li, L., and Li, Y. (2010). A one-step method to fabricate PLLA scaffolds with deposition of bioactive hydroxyapatite and collagen using ice-based microporogens. Acta Biomater. *6*, 2013–2019.
21. Chen, G., Ushida, T., and Tateishi, T. (2001). Preparation of poly(L-lactic acid) and poly(DL-lactic-co-glycolic acid) foams by use of ice microparticulates. Biomaterials *22*, 2563–2567.
22. Gersbach, C.A., Phillips, J.E., and García, A.J. (2007). Genetic engineering for skeletal regenerative medicine. Annu. Rev. Biomed. Eng. *9*, 87–119.
23. Dai, J., and Rabie, A.B. (2007). The use of recombinant adeno-associated virus for skeletal gene therapy. Orthod. Craniofac. Res. *10*, 1–14.
24. Giacca, M., and Zacchigna, S. (2012). Virus-mediated gene delivery for human gene therapy. J. Control. Release *161*, 377–388.
25. Gu, X., Matsumura, Y., Tang, Y., Roy, S., Hoff, R., Wang, B., and Wagner, W.R. (2017). Sustained viral gene delivery from a micro-fibrous, elastomeric cardiac patch to the ischemic rat heart. Biomaterials *133*, 132–143.
26. Jeon, O., Song, S.J., Kang, S.W., Putnam, A.J., and Kim, B.S. (2007). Enhancement of ectopic bone formation by bone morphogenetic protein-2 released from a heparin-conjugated poly(L-lactic-co-glycolic acid) scaffold. Biomaterials *28*, 2763–2771.
27. Wang, Z., Wang, K., Lu, X., Li, M., Liu, H., Xie, C., Meng, F., Jiang, O., Li, C., and Zhi, W. (2015). BMP-2 encapsulated polysaccharide nanoparticle modified biphasic calcium phosphate scaffolds for bone tissue regeneration. J. Biomed. Mater. Res. A *103*, 1520–1532.
28. Lee, C.H., Jin, M.U., Jung, H.M., Lee, J.T., and Kwon, T.G. (2015). Effect of dual treatment with SDF-1 and BMP-2 on ectopic and orthotopic bone formation. PLoS ONE *10*, e0120051.
29. Yamamoto, M., Tabata, Y., and Ikada, Y. (1998). Ectopic bone formation induced by biodegradable hydrogels incorporating bone morphogenetic protein. J. Biomater. Sci. Polym. Ed. *9*, 439–458.
30. Furuya, Y., Inagaki, A., Khan, M., Mori, K., Penninger, J.M., Nakamura, M., Udagawa, N., Aoki, K., Ohya, K., Uchida, K., et al. (2013). Stimulation of bone formation in cortical bone of mice treated with a receptor activator of nuclear factor-κB ligand (RANKL)-binding peptide that possesses osteoclastogenesis inhibitory activity. J. Biol. Chem. *288*, 5562–5571.
31. Suliman, S., Sun, Y., Pedersen, T.O., Xue, Y., Nickel, J., Waag, T., Finne-Wistrand, A., Steinmüller-Nethl, D., Krueger, A., Costea, D.E., et al. (2016). In vivo host response and degradation of copolymer scaffolds functionalized with nanodiamonds and bone morphogenetic protein 2. Adv. Healthc. Mater. *5*, 730–742.
32. Jiang, Y., Cai, Y., Zhang, W., Yin, Z., Hu, C., Tong, T., Lu, P., Zhang, S., Neculai, D., Tuan, R.S., et al. (2016). Human cartilage-derived progenitor cells from committed chondrocytes for efficient cartilage repair and regeneration. Stem Cells Transl. Med. *5*, 733–744.
33. Xiao, X., Li, J., and Samulski, R.J. (1998). Production of high-titer recombinant adeno-associated virus vectors in the absence of helper adenovirus. J. Virol. *72*, 2224–2232.
34. Wang, B., Li, J., and Xiao, X. (2000). Adeno-associated virus vector carrying human minidystrophin genes effectively ameliorates muscular dystrophy in mdx mouse model. Proc. Natl. Acad. Sci. USA *97*, 13714–13719.
35. Baker, N., Zhang, G., You, Y., and Tuan, R.S. (2012). Caveolin-1 regulates proliferation and osteogenic differentiation of human mesenchymal stem cells. J. Cell. Biochem. *113*, 3773–3787.
36. Bouxsein, M.L., Boyd, S.K., Christiansen, B.A., Guldberg, R.E., Jepsen, K.J., and Müller, R. (2010). Guidelines for assessment of bone microstructure in rodents using micro-computed tomography. J. Bone Miner. Res. *25*, 1468–1486.